Hypothalamic thyroid hormone deficiency underlies reversible anorexia in a mammalian hibernator

Sarah M. Mohr[1,2,3], Rafael Dai Pra[1,2,3], Maryann P. Platt[1,2,3], Viktor V. Feketa[1,2,3], Marya Shanabrough[4], Luis Varela[4,5], Ashley Kristant[4], Haoran Cao [1,2,3], Dana K. Merriman[6], Tamas L. Horvath[4,5], Sviatoslav N. Bagriantsev[1*], and Elena O. Gracheva[1,2,3*]

[1]Department of Cellular and Molecular Physiology, Yale University School of Medicine, 333 Cedar Street, New Haven, CT 06510, USA

[2]Department of Neuroscience, Yale University School of Medicine, 333 Cedar Street, New Haven, CT 06510, USA

[3]Kavli Institute for Neuroscience, Yale University School of Medicine, 333 Cedar Street, New Haven, CT 06510, USA

[4]Department of Comparative Medicine, Yale University School of Medicine, 310 Cedar Street, New Haven, CT 06510, USA.

[5]Achucarro Basque Center for Neuroscience, Leioa, Spain 48940

[6]Department of Biology, University of Wisconsin-Oshkosh, 800 Algoma Boulevard, Oshkosh, WI 54901, USA

*Correspondence: slav.bagriantsev@yale.edu and elena.gracheva@yale.edu

Abstract

Mammalian hibernators survive prolonged periods of cold and resource scarcity by temporarily modulating normal physiological functions, but the mechanisms underlying these adaptations are poorly understood. The hibernation cycle of thirteen-lined ground squirrels lasts for 5–7 months and comprises weeks of hypometabolic, hypothermic torpor interspersed with 24–48-hour periods of an active-like interbout arousal (IBA) state. We show that ground squirrels, who endure the entire hibernation season without food, have negligible hunger drive during IBAs. These squirrels exhibit reversible inhibition of the hypothalamic feeding center, such that hypothalamic arcuate nucleus neurons exhibit reduced sensitivity to the orexigenic and anorexigenic effects of ghrelin and leptin, respectively. However, hypothalamic infusion of thyroid hormone during an IBA is sufficient to rescue hibernation anorexia. Our results reveal that thyroid hormone deficiency underlies hibernation anorexia and demonstrate the functional flexibility of the hypothalamic feeding center.

31 Hibernation was first documented in 350 BCE by Aristotle, who noted that some creatures
32 cease eating and conceal themselves in a sleep-like state for many months to pass the winter[1].
33 Hibernation invokes a series of flexible adaptations that allow animals to thrive in inhospitable
34 environments, where they experience thermal challenges and food scarcity[2]. Coordination of
35 hunger and satiety is essential for hibernators to survive, as premature emergence from
36 underground burrows to seek food may dysregulate dependent processes and increase the risk
37 of predation.
38 In thirteen-lined ground squirrels *(Ictidomys tridecemlineatus)*, hibernation consists of repeated
39 cycles of hypothermic torpor interspersed with brief periods of euthermic IBA (Fig. 1a, b). During
40 torpor, animals enter a state of suspended animation by profoundly reducing their metabolic,
41 heart and respiration rates, and lowering their body temperature to 2–4 °C. Every 2–3 weeks,
42 squirrels arouse to spend ~24 hours in IBA, when their main bodily functions temporarily return
43 to an active-like state (Fig. 1b)[3]. Ground squirrels do not depend on stored food for fuel during
44 hibernation; instead, energy is supplied by body fat amassed during the summer. Thus, although
45 hibernating squirrels resemble fasted animals metabolically, they demonstrate little interest in
46 food despite enduring over seven months of starvation[4–7]. We sought to understand the
47 mechanism underlying this remarkable example of reversible anorexia by comparing euthermic
48 animals during the active season with euthermic animals during IBAs in the hibernation season.
49 These experiments reveal that thyroid hormone deficiency in the hypothalamus underlies
50 hibernation anorexia.
51

52 ## Results

53 ### Hibernating ground squirrels have negligible hunger drive

54 When squirrels were presented with food during the numerous IBAs throughout the hibernation
55 season, they consumed approximately six times less food than during the active state (active:
56 14.0 ± 0.8 g/day; IBA: 2.4 ± 0.2 g/day; Fig. 1c). Their body weight continuously decreased
57 throughout hibernation, reaching ~50% of their starting weight by the end of the season (Fig. 1c).
58 During IBAs, we found reduced levels of serum glucose (active: 22.2 ± 2.9 mM; IBA: 12.8 ± 1.1
59 mM) and serum insulin (active: 44.4 ± 7.4 µU/mL; IBA: 8.4 ± 1.3 µU/mL), both of which decreased

60 throughout hibernation (Fig. 1d, e). Consistent with metabolism of fat being the primary energy
61 source during hibernation, squirrels exhibited increased levels of serum β-hydroxybutyrate
62 during IBAs compared to active squirrels (active: 0.23 ± 0.04 mM; IBA: 2.07 ± 0.25 mM; Fig. 1f).
63 Thus, squirrels appear to lack hunger drive during hibernation, even during IBAs.
64

65 **Hibernating squirrels demonstrate reversible resistance to ghrelin**

66 During fasting, the stomach releases the orexigenic hormone ghrelin, which activates Agouti-
67 Related Peptide/Neuropeptide Y (AgRP/NPY) neurons in the arcuate nucleus of the
68 hypothalamus (ARC)[8–12]. To investigate whether low levels of ghrelin underlie lack of hunger in
69 hibernating squirrels, we measured total and active ghrelin in blood plasma. There was no
70 significant difference between IBA and active squirrels, and active ghrelin showed an increasing
71 trend throughout hibernation, albeit insignificant (Fig. 2a-c). Because such high ghrelin levels are
72 sufficient to induce feeding in active animals, we hypothesized that hibernating squirrels develop
73 seasonal ghrelin resistance[4,13]. We tested this by monitoring food consumption in active and IBA
74 squirrels after peripheral injection of ghrelin. As expected, ghrelin potentiated feeding in active
75 squirrels to levels observed in mice and rats[14–16], exceeding those of active squirrels after 48
76 hours of food deprivation (Fig. 2d, e). In stark contrast, ghrelin failed to potentiate food
77 consumption when injected during IBAs (Fig. 2d).

78 Immunohistochemical analysis of *c-FOS* expression showed that ghrelin injections activated
79 a subset of ARC neurons in active, but not IBA, animals (Fig. 2f, g), suggesting that AgRP/NPY
80 neurons have reduced sensitivity to ghrelin during hibernation. In normal physiological
81 conditions, ghrelin binding to growth-hormone secretagogue receptors (*Ghsrs*) on AgRP/NPY
82 neurons triggers release of AgRP from nerve terminals[8,17–21]. In contrast, we observed that AgRP
83 accumulates in neuronal somas during IBAs (Fig. 2h), implying diminished release. Deep
84 sequencing of the ARC showed similar levels of *Ghsrs* in active and IBA animals (Fig. 2i). Moreover,
85 *de novo* cloning of the ARC *Ghsr* revealed that > 95% of transcripts in IBA animals represented
86 the full-length functional *Ghsr* isoform[20] (Fig. 2j). Thus, the absence of a neuronal and behavioral
87 response to peripheral ghrelin injection in IBA squirrels cannot be attributed to a lack of
88 functional ghrelin receptors.

89

90 **Hibernating squirrels have reduced leptin signaling**

91 To investigate whether additional mechanisms are involved in the lack of hunger drive in
92 hibernating squirrels, we asked if ARC neurons are sensitive to the satiety hormone leptin during
93 IBAs. Plasma levels of leptin were slightly elevated in IBAs compared to active animals (Fig. 3a).
94 In addition, deep sequencing of the ARC as well as *de novo* cloning revealed active-like levels of
95 expression of both full-length and truncated transcripts of the long isoform leptin receptor
96 (*Lepr*)[22] in IBA animals (Fig. 3b-c). However, despite the presence of leptin and its receptor during
97 hibernation, we observed significantly lower expression of the phosphorylated form of the
98 transcription factor signal transducer and activator of transcription 3 (pSTAT3) – a marker for
99 leptin signaling in neurons[23] – in the ARC of IBA compared to active animals (Fig. 3d-e). These
100 data imply that leptin signaling in ARC neurons is reduced in hibernating squirrels.

101

102 **Hibernating animals demonstrate central hypothyroidism**

103 Our findings that ARC neurons resist the orexigenic effects of ghrelin and exhibit reduced
104 leptin signaling during IBAs suggested that the hypothalamic feeding center temporarily shuts
105 down during hibernation. However, the mechanism responsible for this effect remained unclear.
106 The action of the thyroid hormone triiodothyronine (T3) in the central nervous system (CNS) has
107 been implicated in the control of feeding[24–28]. It has further been shown that the excitability of
108 ARC AgRP/NPY neurons during fasting or ghrelin administration is increased via uncoupling
109 protein 2 (UCP2)-dependent mitochondrial proliferation[29,30]. We therefore hypothesized that
110 anorexia during IBA may be due to central T3 deficiency. In support of this, we found more than
111 two-fold lower levels of hypothalamic T3 during IBA compared to active animals (active: 0.77 ±
112 0.1 pg/mg tissue; IBA: 0.32 ± 0.05 pg/mg tissue). Interestingly, we also detected a steady decline
113 in hypothalamic T3 during the active season, reaching levels comparable to those observed
114 during IBA by the end of the season (Fig. 4a). However, plasma levels of T3 were equivalent in
115 both groups of animals and remained constant (Fig. 4b), indicating that thyroid hormone
116 deficiency during hibernation was restricted to the CNS. We also found significantly higher blood
117 serum levels of thyroxine (T4) – the precursor to T3 – during IBA (Fig. 4c), further supporting the

118 idea that hibernating squirrels exhibit central, but not peripheral, hypothyroidism. Thyroid
119 hormones canonically exert their action by binding to nuclear thyroid hormone receptors alpha
120 (*THRA*) and beta (*THRB*)[31]. Single-cell sequencing of ARC neurons revealed that THRA and THRB
121 are expressed in AgRP- and pro-opiomelanocortin (POMC)-containing neurons (Fig. 4d), and that
122 their expression levels are similar in both physiological states (Fig. 4e), suggesting that
123 hypothyroidism in IBA animals is not caused by receptor downregulation. Together, these data
124 indicate that central T3 deficiency may underlie the temporary anorexia associated with
125 hibernation.
126
127 **Central T3 infusion rescues hibernation anorexia**
128 Given the difference between peripheral and central levels of T3, we wondered whether
129 blood brain barrier (BBB) function might be impaired during hibernation. However, 3 kDa dextran
130 and biocytin injections confirmed that ARC BBB function is equivalent in active and IBA animals
131 (Fig. 5a, b and Extended Figure 1). Differential transcriptomics in the ARC subsequently revealed
132 a significant downregulation of monocarboxylate transporter 8 (MCT8) – the thyroid hormone
133 transporter – in IBA animals (Fig. 5c). Because MCT8 participates in the translocation of both T4
134 and T3 from the circulation to brain tissue, and then into glial cells and neurons[32–34], we
135 hypothesized that hypothalamic T3 deficiency may be due to diminished transport of T3 and T4
136 into the ARC. To test this theory, we bypassed this transport step by infusing T3 directly into the
137 mediobasal hypothalamus during IBA and measured its effect on feeding (Fig. 5a). Remarkably,
138 even though T3 injection failed to induce feeding up to two hours post-injection (Fig. 5e), it
139 resulted in robust potentiation of feeding over a 24-hour period (Fig. 5f), consistent with its role
140 as a transcriptional regulator. Thus, the specific deficiency of T3 in the CNS appears to be the
141 cause of hibernation anorexia.
142
143 **Discussion**
144 Anorexia is a severe disorder that impacts quality of human life and can cause death if
145 symptoms are severe. In humans, it can be triggered by lack of hunger, for example during cancer
146 cachexia, or in the psychiatric condition anorexia nervosa, in which subjects self-limit eating

147 despite of hunger. However, anorexia is also part of a normal physiological cycle for ground
148 squirrels, who do not rely on stored food during hibernation. Because premature emergence
149 from the safety of the underground burrow to search for food would pose a risk of predation,
150 anorexia constitutes an important safety mechanism that increases survival. In this study, we
151 found that squirrels exhibit T3 deficiency in the hypothalamus during IBA, and that restoration of
152 T3 reverses anorexia, demonstrating that long-term suppression of hunger during hibernation is,
153 at least partially, due to central hypothyroidism. Thyroid hormone deficiency is specific to the
154 CNS and does not affect peripheral levels of T3 and T4, obviating the adverse effects of
155 hypothyroidism on internal organs[35,36] and preserving the involvement of thyroid hormones in
156 increasing thermogenic capacity prior to squirrels entering hibernation.

157 Hibernating squirrels present a naturalistic model in which central thyroid hormone
158 function is depressed while essential peripheral thyroid function is preserved. Central thyroid
159 hormone has been implicated in the seasonal shifts in reproduction and food intake in non-
160 hibernating animals, including Siberian hamsters, sheep, photoperiodic F344 rats[37–40] and
161 hibernating arctic ground squirrels[41]. Although the precise mechanism of central hypothyroidism
162 remains to be determined in our model, the data presented here suggest that reduced levels of
163 MCT8 may underlie hypothalamic thyroid hormone deficiency during hibernation. Future studies
164 will provide clues to understand the contribution of neurophysiological pathways, including
165 hormone transport, to human anorexia.

166 **Acknowledgements**

167 We thank Lyle Murphy for technical assistance, and members of the Gracheva and Bagriantsev
168 laboratories for comments and critique throughout the study. We thank Dr. Rachel Perry for
169 performing the Leptin ELISA.

170 **Funding.** This work was funded by a Gruber Foundation Fellowship (SMM), The Kavli Foundation
171 (MPP), National Institutes of Health grants R01NS097547 (SNB), and National Science Foundation
172 grants 1923127 (SNB) and 1754286 (EOG). RDP was supported by a scholarship from
173 Coordenação de Aperfeiçoamento de Pessoal de Nível Superior (CAPES), Brazil.

Author contributions. Conceptualization: SMM, EOG, SNB. Data collection: SMM, RDP, MPP, VF, MS, LV, AK, HC, TLH. DKM supplied squirrels and provided advice on animal husbandry. Funding acquisition, project administration and supervision: EOG and SNB. Writing: SMM, RDP, EOG, SNB, TLH with contribution from DKM, MPP, HC.

Competing Interests. Authors declare that they have no competing interests.

Data and materials availability. All data are available in the main text or the supplementary materials. RNA sequencing data are deposited to the Gene Expression Omnibus, accession number XXXX. Single cell RNA sequencing data are deposited to the to the Gene Expression Omnibus, accession number XXXX.

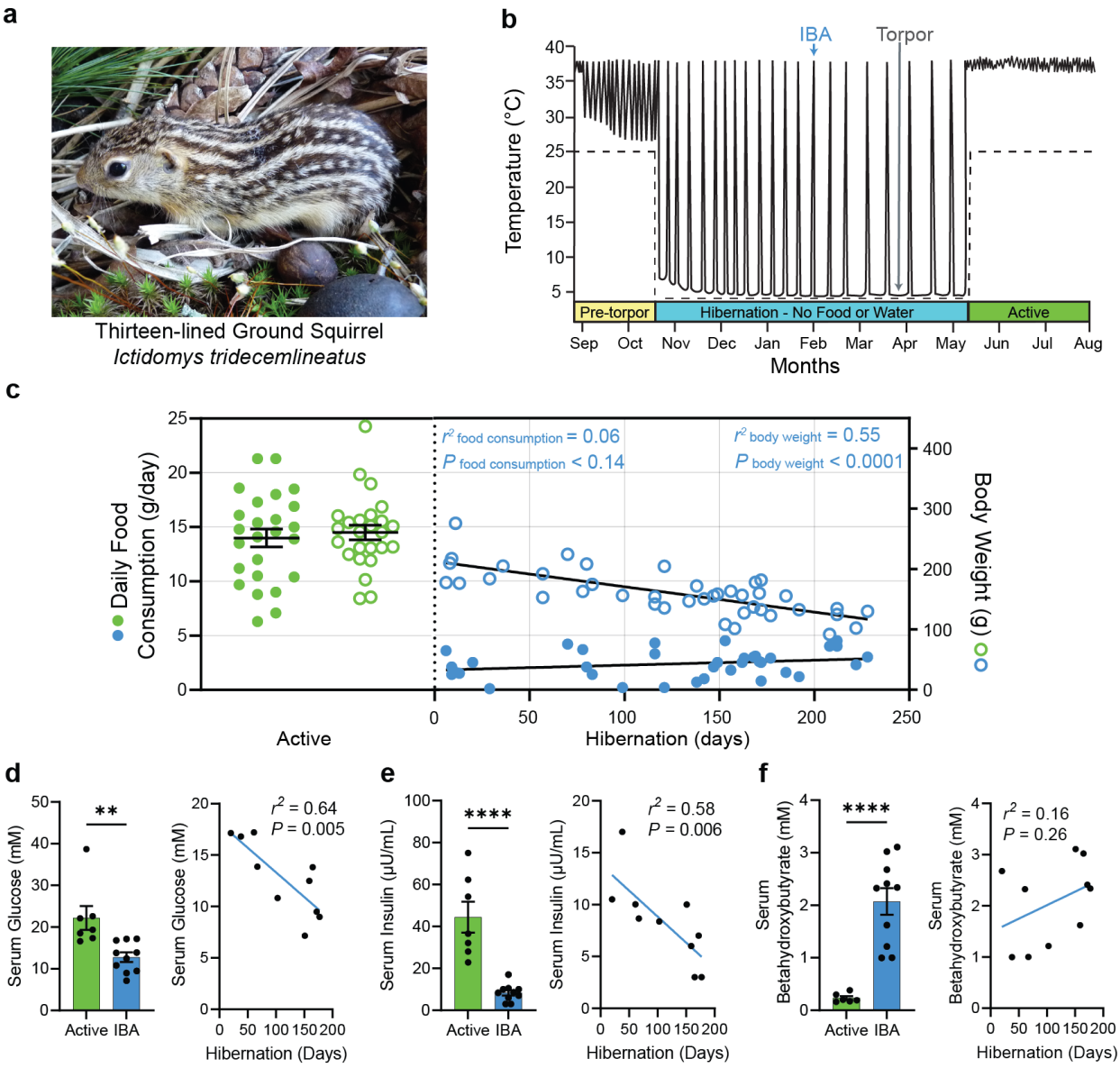

Figure 1: Hibernating ground squirrels have negligible hunger drive.

a, Image of a thirteen-lined ground squirrel, *Ictidomys tridecemlineatus.*

b, Schematic of ground squirrel core body temperature before, during and after hibernation. Dotted line, ambient temperature. Every temperature peak during hibernation represents an IBA.

c, Daily food consumption (left axis, solid points) and body weight (right axis, open circles) during the active (summer) season (green) and hibernation (winter) season (blue). Active feeding data is peak summer food consumption. N = 25 animals. Hibernation feeding and body weight is plotted by days in hibernation. $N_{IBA(Food)}$ = 36, $N_{IBA(Weight)}$ = 42 animals.

d *to* **f**, Blood metabolic indicators across active and hibernation states.

d, Serum glucose, N_{Active} = 7, N_{IBA} = 10 animals. **e**, Serum insulin, N_{Active} = 7, N_{IBA} = 10 animals. **f**, Serum beta-hydroxybutyrate, N_{Active} = 6, N_{IBA} = 10 animals.

Data represent mean ± SEM in histograms. Each point represents one animal. Student's t-test. Scatter plots are the same data plotted against days in hibernation and fitted with simple linear regressions. $^{**}P < 0.01$, $^{****}P < 0.0001$.

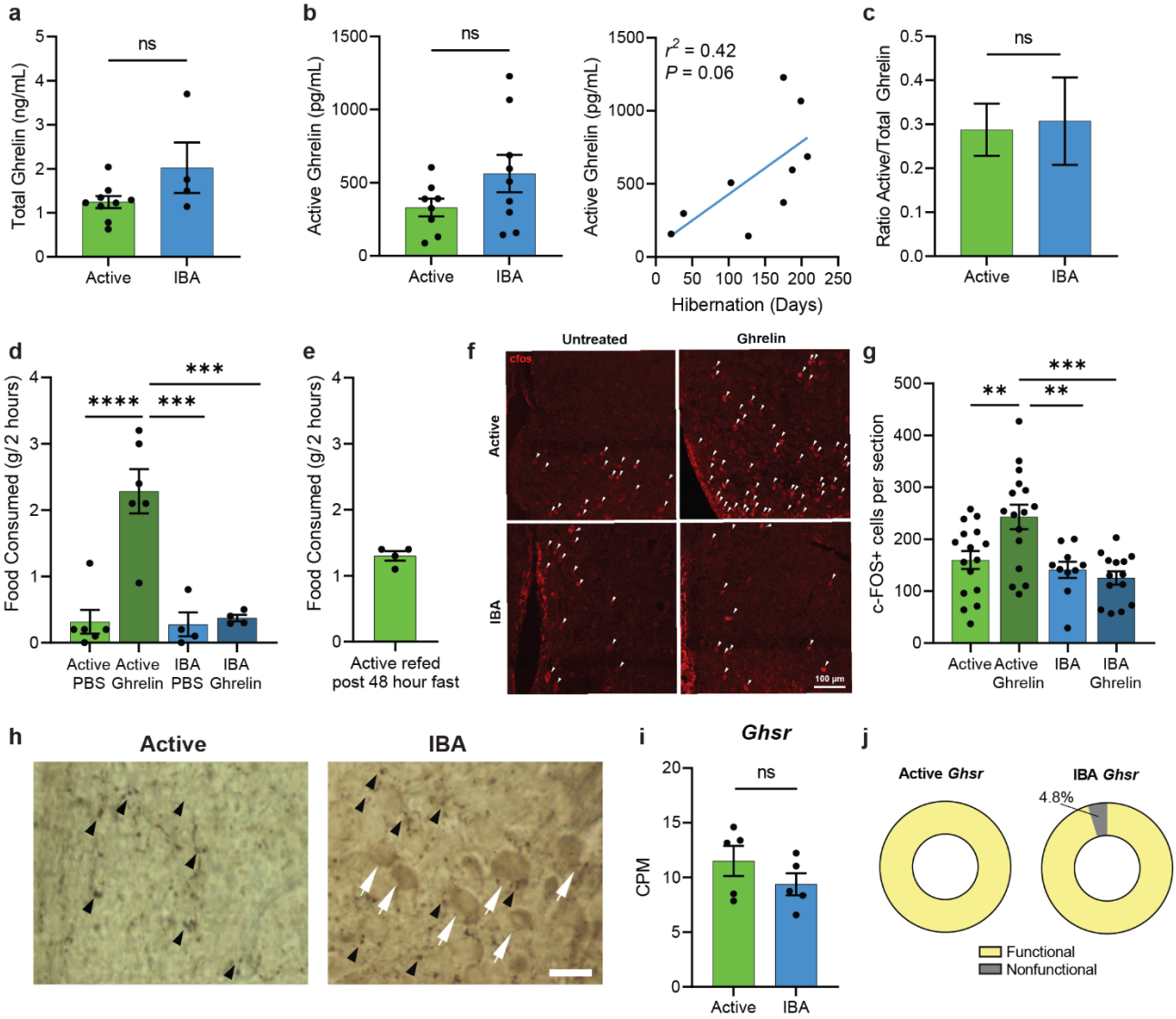

Figure 2: Hibernating squirrels demonstrate reversible resistance to ghrelin.
a, Plasma level of total and **b**, active (acylated) ghrelin across states *(left)* and throughout hibernation *(right)*. Total Ghrelin: $N \geq 4$ animals. Active Ghrelin: $N \geq 8$ animals. **c**, Ratio of active:total ghrelin. **d**, Two-hour food consumption after ghrelin or PBS injection across states. $N \geq 4$ animals.
e, Two-hour food consumption in active animals following 48-hour fast. $N = 4$ animals.
f, Representative images of ARC c-FOS staining of active and IBA squirrels injected with ghrelin or control. Arrowheads, c-FOS+ cells. Scale bar = 100 µm. **g**, Quantification of c-FOS+ cells per section across ARC volume. $N \geq 10$ sections, ≥ 2 squirrels.
h, Representative immuno-EM images of ARC from active and IBA animals. White arrows, neuronal soma; black arrowheads, fibers stained for AgRP. Scale bar = 20 µm.
i, Expression of *Ghsr* in the ARC. $N = 5$ animals.
j, Quantification of *Ghsr* isoforms across states. $N \geq 38$ clones, 2 squirrels.
(**a** – **i**) Data represented as mean ± SEM (**a** – **c**) Student's t-test. $^{**}P < 0.01$, $^{***}P < 0.001$, $^{***}P < 0.0001$. (**d**, **g**) Two-Way ANOVA followed by Tukey's multiple comparisons. $^{**}P < 0.01$, $^{***}P < 0.001$. (**a** – **e**, **i**) Each point represents one animal. (**g**) Each point represents one section. (**i**) $FDR > 0.05$. n.s. = not significant.

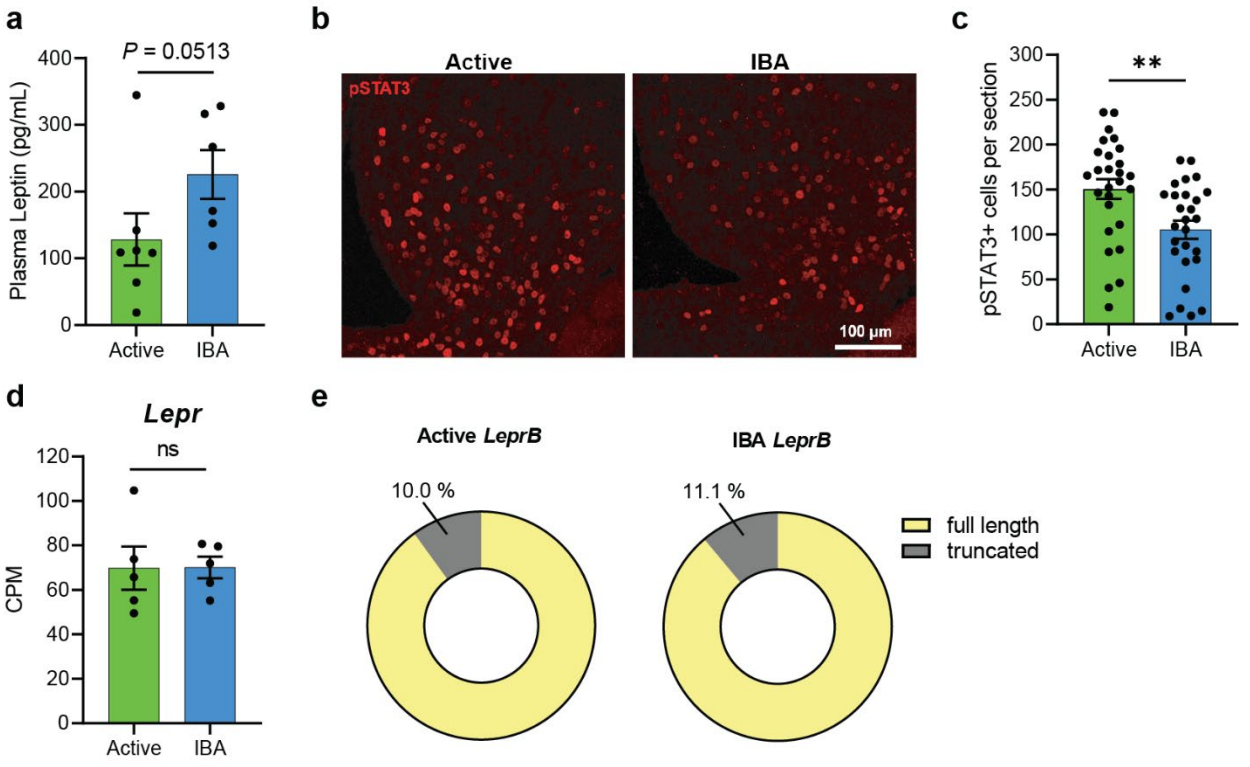

Figure 3: Hibernating squirrels have reduced leptin signaling.

a, Plasma leptin levels across states. Data are mean ± SEM. Mann-Whitney test, N_{Active} = 7 squirrels, N_{IBA} = 6 squirrels.

b, Expression level of *Lepr* in the ARC. Each point represents one squirrel. Data are mean ± SEM, *FDR* > 0.05, ns = not significant. N_{Active} = 5, N_{IBA} = 5.

c, Quantification of truncated versus full length long-form leptin receptor from full-length de novo cloning in active and IBA squirrels. N_{Active} = 10 clones from 2 squirrels, N_{IBA} = 9 clones from 2 squirrels.

d, Representative immunohistochemistry images of ARC in active and IBA squirrels using anti-pSTAT3 antibody. Scale bar, 100 µm.

e, Quantification of pSTAT3+ cells per section by state across ARC volume. Each point represents one section. Data are mean ± SEM. Student's t-test, $P < 0.01$, N_{Active} = 27 sections from 3 squirrels; N_{IBA} = 27 sections from 3 squirrels.

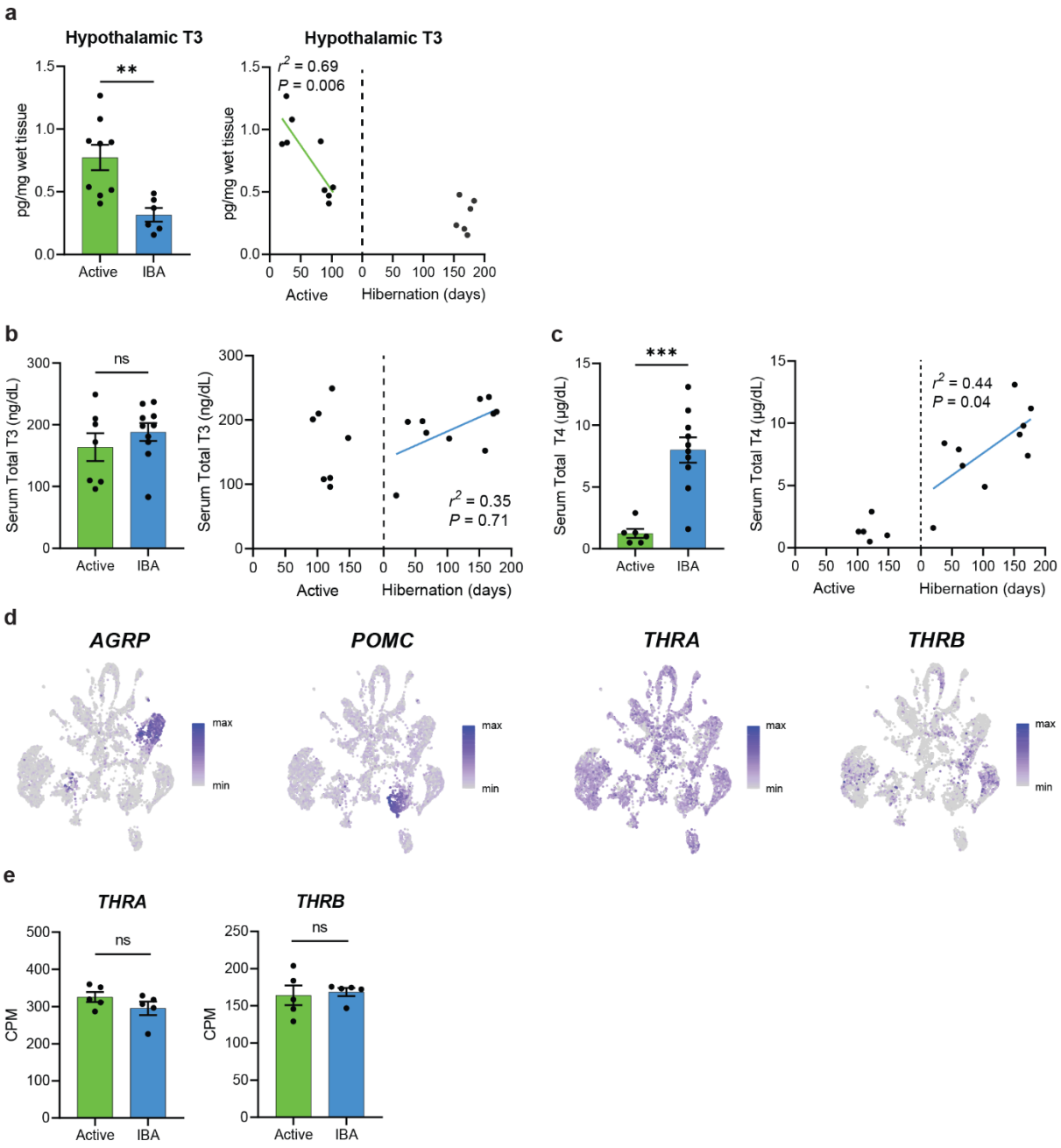

Figure 4: Hibernating animals demonstrate central hypothyroidism.

a, T3 content measured from homogenized hypothalamus from active and IBA squirrels. N_{Active} = 9, N_{IBA} = 6 animals.

b *to* **c**, Serum total thyroid hormone concentration across active and IBA seasons. **b**, Total T3. N_{Active} = 7, N_{IBA} = 10 animals. **C** Total T4 . N_{Active} = 6, N_{IBA} = 10 animals.

d, Single cell sequencing shows clusters expressing *Agrp, Pomc, Thra, Thrb. N* = 3 animals .

e, Transcript expression of *Thra* and *Thrb* assessed by RNA sequencing of ARC. N_{Active} = 5, N_{IBA} = 5 animals. (**a** – **c**) Data represent mean ± SEM in histograms. Each point represents one animal. Student's t-test. ***P* < 0.01, ****P* < 0.001, n.s. = not significant. The same data are plotted against days active and days in hibernation and fitted with simple linear regression. (**e**) *FDR* > 0.05, n.s. = not significant. Data represent mean ± SEM. Each point represents one animal.

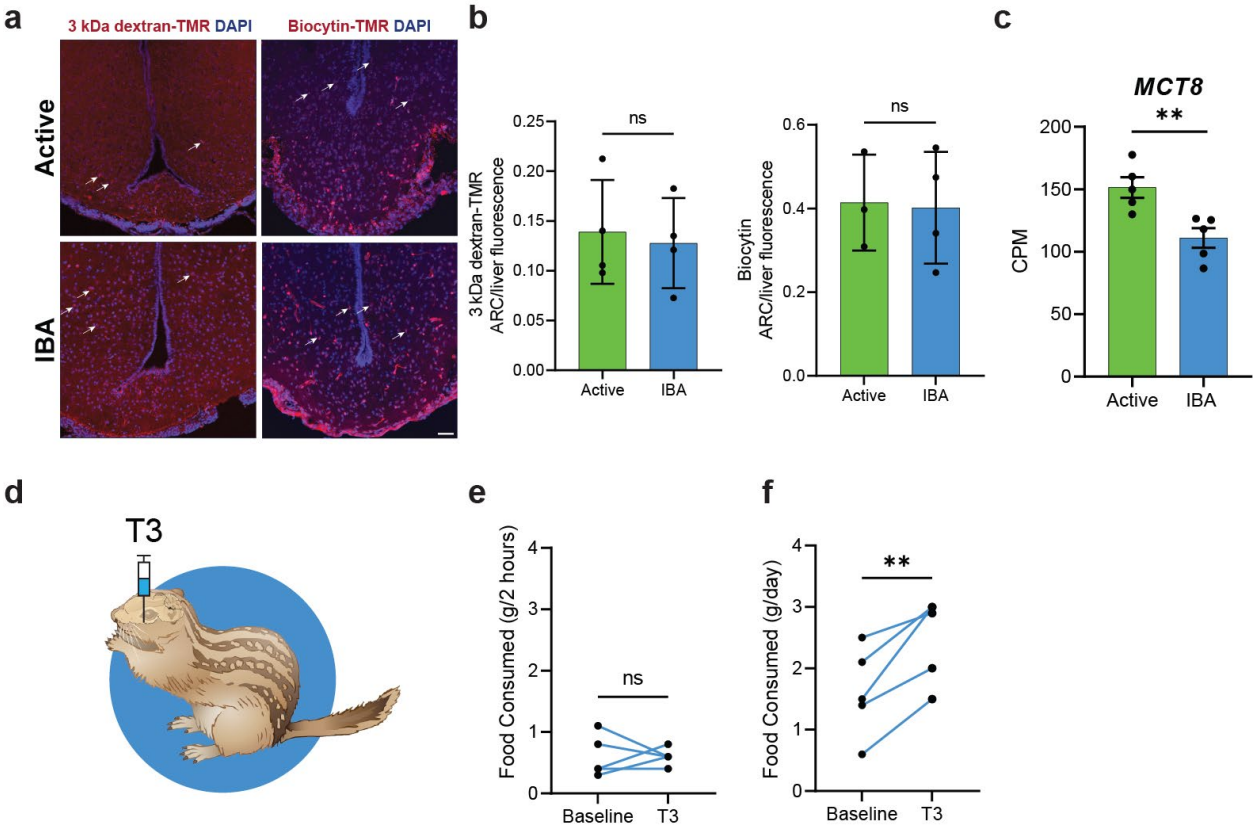

Figure 5: Central T3 infusion rescues hibernation anorexia.

a *to* **b**, Blood brain permeability assays by tail artery injection in active and IBA squirrels of 3kDa dextran-tetramethylrhodamine (TMR) and 860 Da biocytin-TMR results in **a**, deposition of dye (white arrows) within the median eminence and ARC. Scale bar = 50 µm. **b**, Quantification of normalized fluorescence of 3kDa TMR (left) and 860 Da biocytin-TMR (right). Dextran: N_{Active} = 4, N_{IBA} = 4 animals. Biocytin: N_{Active} = 3, N_{IBA} = 4 animals. **c**, Level of expression of *MCT8* in the ARC. N_{Active} = 5, N_{IBA} = 5 animals. **d** *to* **f**, Hypothalamic infusion of T3 during IBA and resulting food consumption. **d**, Schematic of hypothalamic T3 infusion during IBA after arousal from torpor. **e** *to* **f**, Paired food consumption at baseline and after T3 infusion at **e**, two-hours and **F** 24-hours. *N* = 5 animals.

(**b** – **c**) Data represent mean ± SEM. Each point represents one animal. (**b**) Student's t-test. n.s. = not significant. (**c**) ***FDR* < 0.01. (**e** – **f**) Data are paired with each point representing one animal. Student's Paired t-test. ***P* < 0.01; n.s. = not significant. *P* > 0.05.

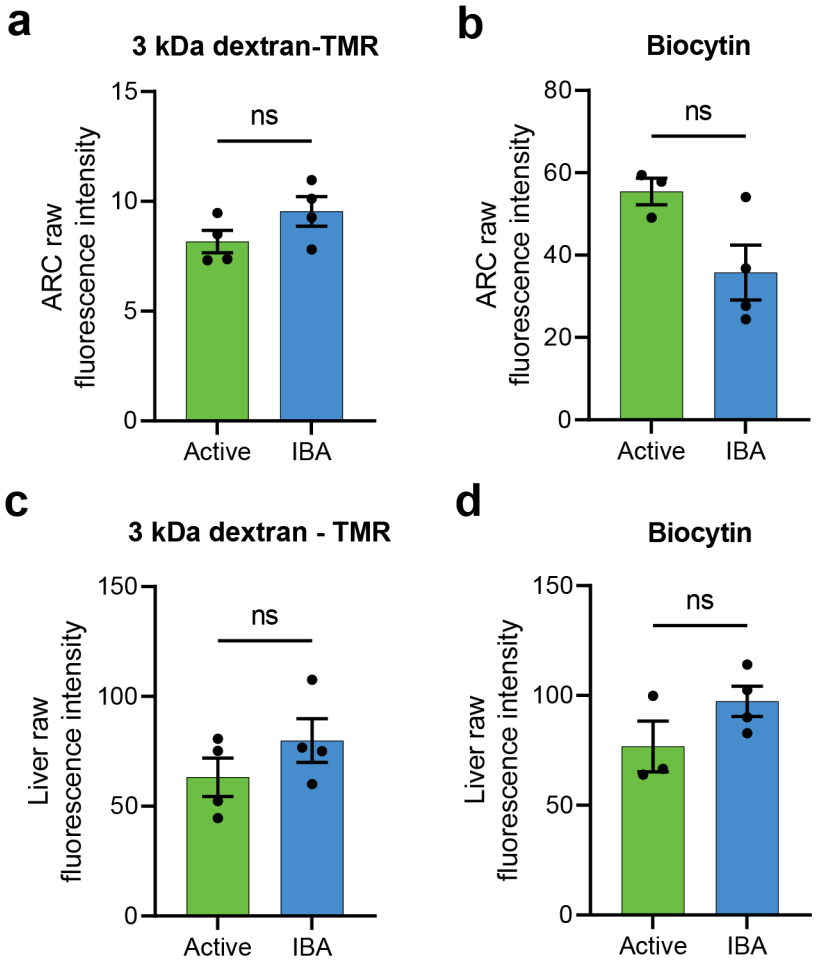

Extended Figure 1: Raw fluorescence intensity of dyes.
Quantification of raw fluorescence intensity for 3kDa dextran-TMR and biocytin-TMR in **a** *to* **b**, ARC and **c** *to* **d,** liver. Data represent mean ± SEM with each point representing one animal. $N \geq 3$ per group. Student's t-test. $P > 0.05$. n.s. = not significant.

References

1. Aristotle. *The History of Animals*. vol. Book 8, Part 13-17 (The Internet Classics Archive, 350AD).
2. Mohr, S. M., Bagriantsev, S. N. & Gracheva, E. O. Cellular, Molecular, and Physiological Adaptations of Hibernation: The Solution to Environmental Challenges. *Annu. Rev. Cell Dev. Biol.* **36**, 315–338 (2020).
3. Andrews, M. T. Molecular interactions underpinning the phenotype of hibernation in mammals. *J. Exp. Biol.* **222**, jeb160606 (2019).
4. Healy, J. E., Bateman, J. L., Ostrom, C. E. & Florant, G. L. Peripheral ghrelin stimulates feeding behavior and positive energy balance in a sciurid hibernator. *Horm. Behav.* **59**, 512–519 (2011).
5. Mrosovsky, N. & Boshes, M. Meal patterns and food intakes of ground squirrels during circannual cycles. *Appetite* **7**, 163–175 (1986).
6. Torke, K. G. & Twente, J. W. Behavior of Spermophilus lateralis between Periods of Hibernation. *J. Mammal.* **58**, 385–390 (1977).
7. Pulawa, L. K. & Florant, G. L. The Effects of Caloric Restriction on the Body Composition and Hibernation of the Golden-Mantled Ground Squirrel (Spermophilus lateralis). *Physiol. Biochem. Zool.* **73**, 538–546 (2000).
8. Cowley, M. A. *et al.* The Distribution and Mechanism of Action of Ghrelin in the CNS Demonstrates a Novel Hypothalamic Circuit Regulating Energy Homeostasis. *Neuron* **37**, 649–661 (2003).
9. Gropp, E. *et al.* Agouti-related peptide–expressing neurons are mandatory for feeding. *Nat. Neurosci.* **8**, 1289–1291 (2005).
10. Hahn, T. M., Breininger, J. F., Baskin, D. G. & Schwartz, M. W. Coexpression of Agrp and NPY in fasting-activated hypothalamic neurons. *Nat. Neurosci.* **1**, 271–272 (1998).
11. Kojima, M. *et al.* Ghrelin is a growth-hormone-releasing acylated peptide from stomach. *Nature* **402**, 656–660 (1999).
12. Toshinai, K. *et al.* Upregulation of Ghrelin Expression in the Stomach upon Fasting, Insulin-Induced Hypoglycemia, and Leptin Administration. *Biochem. Biophys. Res. Commun.* **281**, 1220–1225 (2001).
13. Bradley, S. P., Pattullo, L. M., Patel, P. N. & Prendergast, B. J. Photoperiodic regulation of the orexigenic effects of ghrelin in Siberian hamsters. *Horm. Behav.* **58**, 647–652 (2010).
14. Nakazato, M. *et al.* A role for ghrelin in the central regulation of feeding. *Nature* **409**, 194–198 (2001).
15. Wren, A. M. *et al.* The Novel Hypothalamic Peptide Ghrelin Stimulates Food Intake and Growth Hormone Secretion. *Endocrinology* **141**, 4325–4328 (2000).
16. Asakawa, A. *et al.* Ghrelin is an appetite-stimulatory signal from stomach with structural resemblance to motilin. *Gastroenterology* **120**, 337–345 (2001).
17. Sun, Y., Wang, P., Zheng, H. & Smith, R. G. Ghrelin stimulation of growth hormone release and appetite is mediated through the growth hormone secretagogue receptor. *Proc. Natl. Acad. Sci.* **101**, 4679–4684 (2004).
18. Nogueiras, R. *et al.* Bsx, a Novel Hypothalamic Factor Linking Feeding with Locomotor Activity, Is Regulated by Energy Availability. *Endocrinology* **149**, 3009–3015 (2008).
19. Chen, H. Y. *et al.* Orexigenic Action of Peripheral Ghrelin Is Mediated by Neuropeptide Y and Agouti-Related Protein. *Endocrinology* **145**, 2607–2612 (2004).
20. Yanagi, S., Sato, T., Kangawa, K. & Nakazato, M. The Homeostatic Force of Ghrelin. *Cell Metab.* **27**, 786–804 (2018).
21. Sakkou, M. *et al.* A Role for Brain-Specific Homeobox Factor Bsx in the Control of Hyperphagia and Locomotory Behavior. *Cell Metab.* **5**, 450–463 (2007).
22. Gorska, E. *et al.* Leptin receptors. *Eur. J. Med. Res.* **15**, 50–54 (2010).
23. Vaisse, C. *et al.* Leptin activation of Stat3 in the hypothalamus of wild–type and ob/ob mice but not db/db mice. *Nat. Genet.* **14**, 95–97 (1996).

24. Kong, W. M. *et al.* Triiodothyronine Stimulates Food Intake via the Hypothalamic Ventromedial Nucleus Independent of Changes in Energy Expenditure. *Endocrinology* **145**, 5252–5258 (2004).
25. Varela, L. *et al.* Hypothalamic mTOR pathway mediates thyroid hormone-induced hyperphagia in hyperthyroidism. *J. Pathol.* **227**, 209–222 (2012).
26. Amin, A., Dhillo, W. S. & Murphy, K. G. The Central Effects of Thyroid Hormones on Appetite. *J. Thyroid Res.* **2011**, (2011).
27. Diano, S., Naftolin, F., Goglia, F. & Horvath, T. L. Fasting-Induced Increase in Type II Iodothyronine Deiodinase Activity and Messenger Ribonucleic Acid Levels Is Not Reversed by Thyroxine in the Rat Hypothalamus*. *Endocrinology* **139**, 2879–2884 (1998).
28. Diano, S., Naftolin, F., Goglia, F., Csernus, V. & Horvath, T. L. Monosynaptic Pathway Between the Arcuate Nucleus Expressing Glial Type II Iodothyronine 5′-Deiodinase mRNA and the Median Eminence-Projective TRH Cells of the Rat Paraventricular Nucleus. *J. Neuroendocrinol.* **10**, 731–742 (1998).
29. Coppola, A. *et al.* A Central Thermogenic-like Mechanism in Feeding Regulation: An Interplay between Arcuate Nucleus T3 and UCP2. *Cell Metab.* **5**, 21–33 (2007).
30. Andrews, Z. B. *et al.* UCP2 mediates ghrelin's action on NPY/AgRP neurons by lowering free radicals. *Nature* **454**, 846–851 (2008).
31. Mullur, R., Liu, Y.-Y. & Brent, G. A. Thyroid Hormone Regulation of Metabolism. *Physiol. Rev.* **94**, 355–382 (2014).
32. Wirth, E. K. *et al.* Neuronal 3′,3,5-Triiodothyronine (T3) Uptake and Behavioral Phenotype of Mice Deficient in Mct8, the Neuronal T3 Transporter Mutated in Allan–Herndon–Dudley Syndrome. *J. Neurosci.* **29**, 9439–9449 (2009).
33. Roberts, L. M. *et al.* Expression of the Thyroid Hormone Transporters Monocarboxylate Transporter-8 (SLC16A2) and Organic Ion Transporter-14 (SLCO1C1) at the Blood-Brain Barrier. *Endocrinology* **149**, 6251–6261 (2008).
34. Braun, D. *et al.* Developmental and cell type-specific expression of thyroid hormone transporters in the mouse brain and in primary brain cells. *Glia* **59**, 463–471 (2011).
35. Ettleson, M. D. & Papaleontiou, M. Evaluating health outcomes in the treatment of hypothyroidism. *Front. Endocrinol.* **13**, 1026262 (2022).
36. Fenneman, A. C., Bruinstroop, E., Nieuwdorp, M., van der Spek, A. H. & Boelen, A. A comprehensive review of thyroid hormone metabolism in the gut and its clinical implications. *Thyroid* (2022) doi:10.1089/thy.2022.0491.
37. Barrett, P. *et al.* Hypothalamic Thyroid Hormone Catabolism Acts as a Gatekeeper for the Seasonal Control of Body Weight and Reproduction. *Endocrinology* **148**, 3608–3617 (2007).
38. Herwig, A. *et al.* Photoperiod and acute energy deficits interact on components of the thyroid hormone system in hypothalamic tanycytes of the Siberian hamster. *Am. J. Physiol.-Regul. Integr. Comp. Physiol.* **296**, R1307–R1315 (2009).
39. Murphy, M. *et al.* Effects of Manipulating Hypothalamic Triiodothyronine Concentrations on Seasonal Body Weight and Torpor Cycles in Siberian Hamsters. *Endocrinology* **153**, 101–112 (2012).
40. Dardente, H., Hazlerigg, D. G. & Ebling, F. J. P. Thyroid hormone and seasonal rhythmicity. *Front. Endocrinol.* **5**, 19 (2014).
41. Chmura, H. E. *et al.* Hypothalamic remodeling of thyroid hormone signaling during hibernation in the arctic ground squirrel. *Commun. Biol.* **5**, 1–13 (2022).

Methods:

Animals

All experimental procedures were performed in compliance with the Institutional Animal Care and Use Committee of Yale University (protocol 2021-11497). Thirteen-lined ground squirrels (*Ictidomys tridecemlineatus*; age 0.5 – 3 years) of both sexes were single housed in temperature- and humidity-controlled facilities at Yale University. All squirrels were implanted with an interscapular temperature transponder (IPTT-300, BMDS).

During the active season (May – August), squirrels were kept at 20 °C under a 12 hour:12 hour light:dark cycle at 40 – 60% humidity and maintained on a diet of dog food (IAMS) supplemented with sunflower seeds, superworms, and fresh vegetables (celery and carrots) with *ad libitum* access to water.

During hibernation (September – April), hypothermic squirrels (body temperature ~20 °C) were moved to 4 °C at 40 – 60% humidity under constant darkness, without access to food or water. In this study, "active" squirrels were those with a constant core body temperature (CBT) of 37 °C during the active season. "IBA" squirrels were those who had undergone at least one bout of hypothermic torpor during the hibernation season, but had achieved a CBT of > 32 °C for ≥ 60 minutes, or ≥ 20 minutes for the central thyroid hormone experiments.

Food Consumption and Body Mass Measurement

Food consumption and body weight of active adult animals (n = 25) were measured every 2 weeks during the active period (May-August). Active animals were moved to the behavioral room kept at 20 °C under a 12 hour :12 hour light:dark cycle and acclimated overnight. In the morning (9 – 11 AM), each was weighed, transferred to a clean cage, and allowed to habituate for 30 minutes. Food consumption measurements were performed with dog food only. Pre-weighed food was added to each cage, and animals were allowed to feed undisturbed. Food remaining 24 hours later was weighed and used to calculate daily food consumption. A separate bowl of dog food was kept in the behavior room to control for weight changes due to ambient humidity, but no difference was found so no correction was needed. The maximum food consumption per animal for the active season was reported.

Hibernating animals entered IBA spontaneously, so their food consumption and body weight measurements occurred between 11 AM – 8 PM. IBA animals were weighed, transferred to a clean cage in the hibernaculum kept at 4 °C under constant darkness and allowed to habituate for 30 minutes. Food consumption measurements were performed with dog food only. Pre-weighed food was added to each cage, and animals were allowed to feed undisturbed. Food remaining 24 hours later was weighed and used to calculate daily food consumption. IBA measurements occurred just once during the hibernation season, to ensure that animals remained naïve to food availability during the winter. A separate bowl of dog food was kept in the behavior room, kept at 4 °C in constant darkness, to control for weight changes due to ambient humidity, but no difference was found so no correction was needed.

Blood collection

Animals were euthanized by isoflurane overdose. The chest cavity was opened, the right atrium of the heart pierced, and trunk blood was collected with a 18G needle and syringe.

Serum hormone and metabolite measurements

419 Whole blood was allowed to coagulate at room temperature for 30 minutes, then centrifuged at
420 4 °C at 2000 rcf for 15 minutes. Serum was aliquoted and stored at -80 °C for later use. Serum glucose
421 (Active: n = 7; IBA: n = 10), insulin (Active: n = 7; IBA: n = 10), beta-hydroxybutyrate (Active: n = 6; IBA: n =
422 10), total T3 (Active: n = 7; IBA: n = 10), and total T4 measurement (Active: n = 6; IBA: n = 10) were
423 performed by Antech Diagnostics (Fountain Valley, CA).

424 **Plasma ghrelin measurements**

425 Whole blood was collected into chilled, pre-coated K_3EDTA tubes (MiniCollect, Grenier Bio-One)
426 and immediately treated with Pefabloc (Sigma) to a final concentration of 1 mM. Blood was centrifuged
427 at 1600 rcf for 15 minutes. Plasma was aliquoted and stored at -80 °C for later use. Plasma active (acylated)
428 ghrelin (Active: n = 8; IBA: n = 9) was measured by mouse/rat ELISA (EZRGRA-90K, Millipore). Plasma total
429 ghrelin (Active: n = 9; IBA: n = 4) was measured by mouse/rat ELISA (EZRGRT-91K, Millipore). All samples
430 were run in duplicate. The ratio of active (acylated)/ total ghrelin was calculated by dividing the mean of
431 the active (acylated) ghrelin concentration by the mean of the total ghrelin concentration per state. The
432 SEM of the ratio was calculated by simple error propagation given by the formula:

433 $\sigma_{ratio} = sqrt\ ((\sigma A/A)2\ +\ (\sigma B/B)2\ ))\ *\ A/B$

434 where A and B are mean values of active (acylated) and total ghrelin, respectively.

435 **Plasma leptin measurements**

436 Whole blood was collected into chilled, pre-coated K_2EDTA tubes (BD Vacutainer, Lavender/H)
437 and immediately treated with aprotinin (Millipore Sigma, 9087-70-1) to a final concentration of 0.02 mM.
438 Blood was centrifuged at 1600 rcf for 15 minutes. Plasma was aliquoted and stored at -80 °C for later use.
439 Plasma leptin (Active: n = 7, IBA: n = 6) was measured by mouse/rat ELISA (R&D Systems, MOB00). All
440 samples were run in duplicate. A ROUT outlier test (Q = 1 %) was run to identify one outlier in the Active
441 state and two outliers in the IBA state.

442 **Intraperitoneal Ghrelin injections**

443 Ground squirrels were acclimated in the behavioral room overnight. Animals were weighed,
444 transferred to clean cages, and allowed to habituate for 30 minutes. Squirrels were immobilized with
445 decapicones, injected with 2 mg/kg active (acylated) rat ghrelin (1465, Tocris) solubilized in PBS using an
446 injection volume of 2 mL/kg body weight, and returned to their cages. Control injections were PBS injected
447 at a volume of 2 mL/kg body weight. Pre-weighed food was added to the cage and animals allowed to
448 feed for two hours. The food remaining after the feeding period was weighed and used to calculate food
449 consumption.

450 **Immunohistochemistry**

451 Ground squirrels were deeply anesthetized by isoflurane inhalation and then subjected to
452 intracardiac perfusion with PBS followed by fixative [4 % paraformaldehyde in PBS]. Brains were post-
453 fixed overnight, and transferred to serial 10 %, 20 %, 30 % sucrose solutions after sinking. Brains were
454 embedded in OCT, frozen on dry ice, and stored at -80 °C until use. Coronal brain sections of the arcuate
455 nucleus were cut at a thickness of 40 µm on a cryostat (Leica, CM3050S). Sections were mounted onto
456 SuperFrost Plus slides and stored at -80 °C with desiccant until the day of the immunohistochemistry
457 procedure. Sections were dried in an incubator at 37 °C for 30 minutes. Slides were washed three times

458 with PBS for 10 minutes, and then washed with 1 % H2O2 and 1 % NaOH in PBS for 10 minutes. Slides
459 were moved to 0.3 % glycine in PBS 1x for 10 minutes and washed with 0.03 % SDS in PBS. Sections were
460 blocked for two hours at room temperature with 5 % normal goat serum in 0.5 % PBST.

461 For c-FOS immunohistochemistry after ghrelin injection (Active Untreated: n = 2 animals; Active
462 ghrelin: n = 2 animals, 16 sections; IBA Untreated: n = 3 animals, 10 sections; IBA Ghrelin: n = 2 animals,
463 14 sections), sections were incubated with primary antibody (1:500, mouse monoclonal c-FOS C-10, Santa
464 Cruz, sc-271243) at 4 °C for 48 hours. After incubation with the primary antibody, sections were washed
465 four times with 0.1 % PBST for 15 minutes. Sections were incubated with secondary antibody (1:500, Alexa
466 Fluor 647 goat anti-mouse, preadsorbed, Abcam, ab150119) for two hours at room temperature. Sections
467 were washed four times with 0.1 % PBST for 15 minutes, followed by a wash with PBS.

468 For pSTAT3 immunohistochemistry (Active: n = 3, 27 sections; IBA: n = 3, 27 sections), sections
469 were incubated with primary antibody (1:200, rabbit polyclonal Phospho-Stat3 (Tyr705), Cell Signaling
470 Technology, 9131) at 4 °C for 24 hours. After incubation with the primary antibody, sections were washed
471 five times with 0.1 % PBST for 10 minutes. Sections were incubated with secondary antibody (1:1000,
472 Alexa Fluor 555 goat anti-rabbit, Abcam, ab150086) for 2 hours at room temperature. Sections were
473 washed five times with 0.1 % PBST for 15 minutes, followed by a wash with PBS.

474 Slides were mounted using Vectashield with DAPI. Sections were imaged on a Leica SP8 Confocal
475 Microscope at 20X using the LAS X software. Negative controls (primary antibody omitted) were
476 performed for c-FOS and pSTAT3 immunohistochemistry and showed no non-specific fluorescent binding.

477 **Immuno-electron microscopy**

478 Ground squirrels were deeply anesthetized by isoflurane inhalation and were subjected to
479 intracardiac perfusion. Free-floating sections (50 µm thick) were incubated with rabbit anti-AgRP antibody
480 (Phoenix Pharmaceuticals) diluted 1:2000 in 0.1 M PB after 1 hour blocking in 0.1 M PB with 5% normal
481 goat serum. After several washes with PB, sections were incubated in the secondary antibody
482 (biotinylated goat anti-rabbit IgG; 1:250 in PB; Vector Laboratories Inc.) for 2 hours at room temperature,
483 then rinsed several times in PB followed by incubation for 2 hours at room temperature with avidin–
484 biotin–peroxidase (ABC; 1:250 in PB; VECTASTAIN Elite ABC kit PK6100, Vector Laboratories). The
485 immunoreaction was visualized with 3,3-diaminobenzidine (DAB). Sections were then osmicated (1%
486 osmium tetroxide) for 30 minutes, dehydrated through increasing ethanol concentrations (using 1%
487 uranyl acetate in 70% ethanol for 30 min), and flat-embedded in Durcupan between liquid release-coated
488 slides (product no. 70880, Electron Microscopy Sciences). After embedding in Durcupan (14040, Electron
489 Microscopy Sciences), ultrathin sections were cut on a Leica Ultra-Microtome, collected on Formvar-
490 coated single-slot grids, and analyzed with a Tecnai 12 Biotwin electron microscope (FEI) with an AMT XR-
491 16 camera.

492 **Bulk RNA Isolation and Sequencing**

493 Total RNA was isolated from the arcuate nuclei of active (n = 5) and IBA (n = 5) animals that had
494 been deeply anesthetized by isoflurane inhalation and subjected to intracardiac perfusion with ice cold
495 PBS. The brain was rapidly dissected and a vibratome (Leica VT1200) was used to cut 300-600 µm coronal
496 slices posterior to the separation of the optic chiasm. The area surrounding the third ventricle, including
497 the arcuate nucleus and median eminence, were manually dissected out from the slices using 27G needles

498 and placed immediately into RNA lysis buffer from the Quick-RNA Microprep Kit (Zymo, R1050). Total RNA
499 was isolated from tissue using the Quick-RNA Microprep Kit (Zymo, R1050). RNA concentration and
500 integrity number (RIN) were assessed by an Agilent 2100 Bioanalyzer (Agilent, Santa Clara, CA). RNA
501 concentrations were in the range of ~20 – 400 ng/µL and RIN values were in the range of 7.4 – 9.5.

502 Library preparation and sequencing were carried out at the Yale Center for Genome Analysis.
503 Sequencing libraries were prepared using the Kapa mRNA Hyper Prep Kit (Cat# KR1352, Roche) including
504 rRNA depletion. Libraries were sequenced on the Illumina NovaSeq6000 in the 100 bp paired-end mode
505 according to manufacturer's protocols. A total of ~ 22 – 34 million sequencing read pairs per sample were
506 obtained.

507 The sequencing data were processed on the Yale Center for Research Computing cluster. Raw
508 sequencing reads were filtered and trimmed to retain high-quality reads using Trimmomatic v0.39 (*1*) with
509 default parameters. Filtered high-quality reads from all samples were aligned to the *Ictidomys*
510 *tridecemlineatus* reference genome using the STAR aligner v2.7.1a with default parameters (*2*). The
511 SpeTri2.0 [GCA_000236235.1] reference genome and the gene annotation were obtained from the Broad
512 Institute.

513 The gene annotation was filtered to include only protein-coding genes. Aligned reads were
514 counted by the featureCounts programs from the Subread package v2.2.0 with default parameters (*3*).
515 Read counting was performed at the gene level, i.e. the final read count for each gene included all reads
516 mapped to all exons of this gene. Differential expression of genes was determined by EdgeR v 3.32.1 (*4*).
517 Normalized read counts were obtained by normalizing raw read counts to effective library sizes of each
518 sample and expressed as reads/million of total reads in a library (CPM). Statistical analysis was performed
519 using the GLM approach and quasi-likelihood F-test, using a significance value of *FDR* < 0.05.

520 **Primary cell dissociation and single-cell RNA Sequencing.**

521 Primary neurons were isolated from the arcuate nucleus of hypothalamus and median eminence
522 following a published protocol (*5*) with modification (n = 3). Animals were euthanized by isoflurane
523 inhalation overdose followed by cardiac perfusion with brain perfusion solution (containing in mM: 196
524 sucrose, 2.5 KCl, 28 NaHCO3, 1.25 NaH2PO4, 7 Glucose, 1 Sodium Ascorbate, 0.5 CaCl2, 7 MgCl2, 3 Sodium
525 Pyruvate, oxygenated with 95% O2/5% CO2, osmolarity adjusted to 300 mOsm with sucrose, pH adjusted
526 to 7.4). The brain was dissected and slices were cut on a vibratome (Leica, VT1200). A brain slice containing
527 the ARC and ME were identified by the presence of the third ventricle and separation of the optic chiasm.
528 Three successive 600-µm slices containing the ARC were collected. The area around the third ventricle
529 was microdissected from the brain slices using a micro-scalpel (Fine Science Tools, 10055-12).

530 Tissue was digested in Hibernate A medium (custom formulation with 2.5 mM glucose and
531 osmolarity adjusted to 280 mOsm, BrainBits) supplemented with 1 mM lactic acid (Sigma, L1750), 0.5 mM
532 GlutaMAX (ThermoFisher, 35050061) and 2% B27 minus insulin (ThermoFisher, A1895601) containing 20
533 U/ml papain (Worthington Biochemical Corporation, LS003124) in a shaking water bath at 34 °C for 30
534 min and dissociated by mechanical trituration through the tips of glass Pasteur pipettes with decreasing
535 diameter (0.9 mm, 0.7 mm, 0.5 mm, 0.3 mm). Cell suspension was centrifuged over 8% bovine serum
536 albumin (Sigma, A9418-5G) layer. Supernatant was removed leaving ~50 µl of suspension. Cell suspension
537 was resuspended in 950 µl of Hibernate A medium (same formulation as above) and centrifuged at 300
538 rcf for 5 min. Supernatant was removed, leaving ~50 µl of cell suspension, which was gently mixed with a

539 glass pipette and stored on ice. A 10 µl aliquot of cell suspension was mixed with 10 µl of Trypan Blue
540 stain, loaded into a hemocytometer, and used to assess cell concentration and viability.
541 Cell suspension was processed according to the 10X Genomics library preparation protocol at the
542 Center for Genome Analysis/Keck Biotechnology Resource Laboratory at Yale University. Single cell
543 suspension in RT Master Mix was loaded on the Single Cell G Chip and partitioned with a pool of about
544 750,000 barcoded gel beads to form nanoliter-scale Gel Beads-In-Emulsions (GEMs). The volume of cell
545 suspension for loading was calculated based on cell concentration to capture 10,000 cells. Upon
546 dissolution of the Gel Beads in a GEM, the primers were released and mixed with cell lysate and Master
547 Mix. Incubation of the GEMs produced barcoded, full-length cDNA from poly-adenylated mRNA. Silane
548 magnetic beads were used to remove leftover biochemical reagents and primers from the post GEM
549 reaction mixture. Full-length, barcoded cDNA was amplified by PCR to generate sufficient mass for library
550 construction. Enzymatic Fragmentation and Size Selection were used to optimize the cDNA amplicon size
551 prior to library construction. R1 (read 1 primer sequence) was added to the molecules during GEM
552 incubation. P5, P7, a sample index, and R2 (read 2 primer sequence) were added during library
553 construction via End Repair, A-tailing, Adaptor Ligation, and PCR. The final libraries contained the P5 and
554 P7 primers used in Illumina bridge amplification. Sequencing libraries were sequenced on an Illumina
555 NovaSeq instrument with 150 bp reads according to the manufacturer's instructions at the depth of ~1.1-
556 1.4 billion reads/sample.
557
558 Raw sequencing reads were processed using 10X CellRanger v.6.1.2 (10X Genomics, Pleasanton,
559 CA). Custom genome reference for thirteen-lined ground squirrel (*Ictidomys tridecemlineatus*) was built
560 based on the reference genome sequence and annotation obtained from the Ensembl project
561 (www.ensembl.org (*6*) Release 101; all files accessed on 11/20/2020):
562
563 Genome:
564 ftp://ftp.ensembl.org/pub/release-
565 101/fasta/ictidomys_tridecemlineatus/dna/Ictidomys_tridecemlineatus.SpeTri2.0.dna.toplevel.fa.gz
566 Annotation:
567 ftp://ftp.ensembl.org/pub/release-
568 101/gtf/ictidomys_tridecemlineatus/Ictidomys_tridecemlineatus.SpeTri2.0.101.gtf.gz
569
570 The gene annotation was filtered to include only protein-coding genes using cellranger mkgtf. 10X
571 CellRanger was used to obtain transcript read counts for each cell barcode, filtered for cell barcodes called
572 as cells based on the default parameters. Read count matrix was further processed using R 4.2.1, RStudio
573 2022.02.3, and Seurat 4.1.1 (*7*). Non-descriptive ground squirrel gene symbols (i.e. those starting with
574 "ENSSTOG…") were replaced with gene symbols of mouse homolog genes, using the homolog conversion
575 table from Ensembl. Initial set of cells/barcodes was further filtered to include only those with >= 500
576 features/cells, >= UMIs/cells, and <= 10% of mitochondrial genes (defined as those with gene symbol
577 starting with "MT-"). This resulted in ~11,000-20,000 cells/sample included in the dataset for further
578 analysis, with the sequencing depth of ~70-100k reads/cell. Read counts were processed according to the
579 standard Seurat analysis workflow, including normalization, identification of variable features, scaling,
580 PCA, clustering and visualization using tSNE plots. Graphs report normalized gene expression values.
581
582 ***De novo* Receptor Cloning**

583 Total RNA from the arcuate nucleus of animals was collected as described above. The remaining
584 RNA after sequencing was used for *de novo* cloning of *Ghsr* (Active: n = 3; IBA: n = 3) and long-form *Lepr*
585 (Active: n = 2, 1 female; IBA: n = 2). cDNA was prepared (Invitrogen SuperScript III First-Strand Synthesus
586 for RT-PCR, 18080-051) and the gene of interest amplified (Phusion High-Fidelity PCR Kit, E0553S) using
587 the following primers for *Ghsr:* forward 5'- CCAACTTGATCCAGGCTCC -3', reverse 5'-
588 CAAGTTCCGCTGTGCGATGG -3'; and *Lepr:* forward 5'- CAGGTACATGTCTCTGAAGTAAG -3', reverse 5'-
589 GCCACGTGATCCACTATAATAC -3'. Gel electrophoresis was used to isolate the band of interest and DNA
590 extracted using the Qiagen Gel Extraction Kit (28704). ORFs were then ligated to topo vector (StrataClone
591 Blunt PCR Cloning Kit, 240207). cDNA was sent for Sanger Sequencing (Genewiz), and reference sequences
592 compared the NCBI database.

593 **Hypothalamic Infusions**

594 Animals were implanted with abdominal transponders that measured core body temperature,
595 calibrated between 4 – 40 °C (EMKA Technologies, M1-TA) during the active season, while animals were
596 euthermic. Animals were allowed to recover for at least 2 weeks before implanted with hypothalamic
597 infusion cannulas as described below.

598 In a subsequent surgery, infusion cannulas (10 mm 26 G guide, 11 mm 33 G internal, PlasticsOne)
599 were implanted into the mediobasal hypothalamus during the active season while animals were
600 euthermic. Briefly, animals were induced into, and maintained at, a stable anesthesia plane using
601 isoflurane. Animals were administered 0.03 mg/kg preoperative buprenorphine subcutaneously. The
602 scalp was shaved and the animal transferred to a stereotax, where the skin was sterilized by repeated
603 applications of betadine and 70% ethanol. Sterile technique was used to expose the skull and drill a hole
604 to allow for cannula implantation. The following stereotaxic coordinates were utilized for cannula
605 implantation: 0.5 mm posterior bregma, 0.8 mm lateral midline, 8 mm ventral (guide cannula)/9 mm
606 ventral (infusion cannula). Two bone screws (2mm long, 1.2 x 0.25 mm thread, McMaster-Carr) and dental
607 cement (RelyX Unicem Resin, 3M, 56830) were used to anchor the guide cannula to the skull. A dummy
608 cannula was placed in the guide cannula until experiments were performed. Animals received a dose of
609 0.4mg/kg meloxicam in 1.5 mL saline subcutaneously immediately after surgery. Animals received post-
610 operative buprenorphine 0.01 mg/kg and meloxicam 0.2 mg/kg intraperitoneally every 12 hours for 48
611 hours. Animals were allowed to recover for at least 2 weeks before they were hibernated.

612 Two-hour and daily food consumption were measured in paired IBA animals in two separate
613 experiments. In the first experiment, feeding was assessed after baseline (no injection) feeding (n = 5) and
614 triiodothyronine (T3; Sigma, T2877) in the hibernaculum at 4 °C under constant darkness. Control
615 experiments were performed once IBA patterns appeared stabilized and regular (corresponding to IBA 3
616 – 4). Animals were allowed to return to torpor after control experiments. Hypothalamic T3 infusion was
617 performed in the same animals after at least 1 subsequent IBAs had elapsed (corresponding to IBA 5 – 7).

618 In the second experiment, performed in the subsequent year with a new cohort of animals,
619 hypothalamic infusion of DMSO vehicle (control) (n = 6) (Sigma, D2650) and triiodothyronine (T3; Sigma,
620 T2877) in the hibernaculum at 4 °C under constant darkness. Control experiments were performed once
621 IBA patterns appeared stabilized and regular (corresponding to IBA 4 – 12). Animals were allowed to
622 return to torpor after control experiments. Hypothalamic T3 infusion was performed in the same animals
623 after at least 2 subsequent IBAs had elapsed (corresponding to IBA 9 – 15).

624 For both experiments, to reduce stress to the animals, infusions were performed while animals
625 were in the process of arousing from torpor. Animals were identified as IBA candidates when abdominal
626 temperature exceeded 8 °C. Squirrels were weighed and transferred to a clean cage in the hibernaculum,
627 kept at 4 °C in constant darkness. When abdominal temperature exceeded 16 °C and interscapular
628 temperature exceeded 26 °C, a connector assembly consisting of PE50 tubing attached to an infusion
629 cannula was loaded with control DMSO vehicle or 15.3 mM T3 solubilized in DMSO. At this point, animals
630 were responsive to touch, but remained curled in the stereotypical torpor position and were unable to
631 move. An intrahypothalamic dose of either control DMSO or 15.3 nmol T3 was infused in a volume of 1µL
632 over a time span of three minutes. The infusion cannula was allowed to remain in the guide cannula for
633 two minutes to allow for the complete diffusion of the infusion solution The infusion cannula was removed
634 and replaced with a dummy cannula.

635 During this time, animals continued to warm up. Once the abdominal temperature surpassed 28
636 °C and the interscapular temperature surpassed 35 °C, animals became mobile and explored their cages.
637 Animals were allowed to habituate for 20 minutes. The timing of the rewarming process was variable and
638 took on average around 45 minutes. Dog food was exclusively used for feeding consumption
639 measurements. After habituation was complete, a pre-weighed amount of food was placed in the cage.
640 Animals were allowed to feed for 2 hours, at which point the remaining food was removed, weighed, and
641 returned to the cage. Retrieving and weighing the food took less than 10 minutes per animal. The
642 remaining food was returned to the cage and the animal allowed to feed for a further 22 hours, to achieve
643 a 24-hour food consumption measurement.

644 **Hypothalamic Tissue Collection**

645 Naïve animals (Active: n = 9; IBA: n = 6) that had not undergone any experiment were euthanized
646 by isoflurane overdose and perfused with ice-cold PBS. The brain was removed from the skull and a ~6
647 mm thick section collected from the optic chiasm to the mamillary bodies using a rat coronal brain matrix
648 (Electron Microscopy Sciences, 69083-C). The hypothalamus was isolated by removing brain matter above
649 the top of the third ventricle and lateral to the optic tract. Tissue was flash-frozen in liquid nitrogen and
650 stored at -80 °C until processing.

651 **Measurement of Hypothalamic T3**

652 Total triiodothyronine (T3) was extracted from frozen hypothalamus tissue (Active: n = 9; IBA: n =
653 6) and purified as reported previously (*8*). Briefly, hypothalamic tissue was homogenized in 100%
654 methanol containing 1 mM 6-propyl-2-thiouracil (PTU) (Sigma, H34203) in a glass-glass tissue grind pestle
655 (60mm, Kontes, KT885300-0002). Homogenized tissue was centrifuged at 3000 rpm and supernatant
656 removed. The pellet was resuspended and washed twice more in 100% methanol containing 1 mM PTU.
657 T3 was extracted from supernatants and purified through solid-phase chromatography using 200 – 400
658 anion exchange chloride resin (Bio-Rad, 140-1251) in Poly-Prep chromatography columns (Bio-Rad, 731-
659 1550). Columns were developed with 70% acetic acid (Spectrum, AC110) and washed twice with water.
660 Supernatants were passed through the column without vacuum. T3 bound to columns was purified
661 through a series of washes with acetate buffer pH 7.0 and 100% ethanol. T3 was eluted with 2.5 mL 70%
662 acetic acid. Extracts were evaporated to dryness under nitrogen. T3 concentration was measured by ELISA
663 (Leinco Technologies, T181). Dried product was resolubilized in the zero-standard and the kit run
664 according to the manufacturer's instructions.

665 **Blood Brain Barrier Tracer Injections and Analysis**

666 Naïve animals (n = 15) that had not undergone any experiment were anesthetized with isoflurane
667 (4%) in medical air and injected in the tail artery with either biocytin-TMR (ThermoFisher, T12921) or 3kDa
668 dextran-TMR (ThermoFisher, D3307) at 10 mg/kg. Animals were allowed to recover in their home cage
669 for 30 minutes until perfusion fixation with 4% paraformaldehyde as described for
670 Immunohistochemistry.

671 Brains were sectioned on a Leica cryostat at 40 μm and every tenth section was imaged for blood
672 brain barrier permeability analysis. Sections were rinsed with PBS and coverslipped with Vectashield
673 containing DAPI (Vector Labs, H-1200). Z-stack images of liver and arcuate nucleus were acquired on a
674 confocal microscope (Zeiss, LSM-780) using ZEN Software. Maximum intensity projection images were
675 used for quantification in FIJI.

676 **Statistics, analysis, and data collection**

677 Statistical analyses were performed in GraphPad Prism v9.0 or higher (GraphPad Software, San
678 Diego, CA). Final figures were assembled in Adobe Illustrator. Data were tested for normality using the
679 Shapiro-Wilk normality test. When normality was assumed, the Student's t-test was used to compare two
680 groups and Two-Way ANOVA was used to compare multiple groups. Paired data were analyzed with a
681 paired Student's t-test. Tukey's multiple comparisons test was used to find *post hoc* differences among
682 groups. When data were not normal, the Mann-Whitney test was used. Sample sizes and statistical data
683 are reported in the text and figure legends. In the text, values are provided as mean ± SEM, and $P < 0.05$
684 was considered statistically significant. No blinding was used for data collection. Individuals in
685 experimental groups were chosen to best match body weight and to represent both sexes across groups.

686 **Methods References:**

687 1. Bolger, A. M., Lohse, M. & Usadel, B. Trimmomatic: a flexible trimmer for Illumina sequence data.
688 *Bioinformatics* **30**, 2114–2120 (2014).
689 2. Dobin, A. *et al.* STAR: ultrafast universal RNA-seq aligner. *Bioinformatics* **29**, 15–21 (2013).
690 3. Liao, Y., Smyth, G. K. & Shi, W. featureCounts: an efficient general purpose program for assigning
691 sequence reads to genomic features. *Bioinformatics* **30**, 923–930 (2014).
692 4. Robinson, M. D., McCarthy, D. J. & Smyth, G. K. edgeR: a Bioconductor package for differential
693 expression analysis of digital gene expression data. *Bioinformatics* **26**, 139–140 (2010).
694 5. Vazirani, R. P., Fioramonti, X. & Routh, V. H. Membrane Potential Dye Imaging of Ventromedial
695 Hypothalamus Neurons From Adult Mice to Study Glucose Sensing. *J. Vis. Exp. JoVE* 50861 (2013)
696 doi:10.3791/50861.
697 6. Zerbino, D. R. *et al.* Ensembl 2018. *Nucleic Acids Res.* **46**, D754–D761 (2018).
698 7. Hao, Y. *et al.* Integrated analysis of multimodal single-cell data. *Cell* **184**, 3573-3587.e29 (2021).
699 8. Pinna, G. *et al.* Extraction and quantification of thyroid hormones in selected regions and subcellular
700 fractions of the rat brain. *Brain Res. Protoc.* **4**, 19–28 (1999).

701